Marine Pollution Bulletin 194 (2023) 115396

Contents lists available at ScienceDirect

Marine Pollution Bulletin

journal homepage: www.elsevier.com/locate/marpolbul

Investigation of potential metal emissions from galvanic anodes in offshore wind farms into North Sea sediments

Anna Ebeling [a,b,1], Dominik Wippermann [a,b,1], Tristan Zimmermann [a], Ole Klein [a], Torben Kirchgeorg [c], Ingo Weinberg [c], Simone Hasenbein [c], Anna Plaß [c], Daniel Pröfrock [a,*]

[a] Helmholtz-Zentrum Hereon, Institute of Coastal Environmental Chemistry, Department Inorganic Environmental Chemistry, Max-Planck-Str. 1, 21502 Geesthacht, Germany
[b] Universität Hamburg, Department of Chemistry, Inorganic and Applied Chemistry, Martin-Luther-King-Platz 6, 20146 Hamburg, Germany
[c] Federal Maritime and Hydrographic Agency (BSH), Wüstland 2, 22589 Hamburg, Germany

ARTICLE INFO

Keywords:
Multielement analysis
Technology-critical elements
Isotope ratios
German bight
Pollution
Offshore wind energy

ABSTRACT

To evaluate potential metal emissions from offshore wind farms (OWFs), 215 surface sediment samples from different German North Sea OWFs taken between 2016 and 2022 were analyzed for their mass fractions of metals and their isotopic composition of Sr. For the first time, this study provides large-scale elemental data from OWFs of the previously proposed galvanic anode tracers Cd, Pb, Zn, Ga and In. Results show that mass fractions of the legacy pollutants Cd, Pb and Zn were mostly within the known variability of North Sea sediments. At the current stage the analyzed Ga and In mass fractions as well as Ga/In ratios do not point towards an accumulation in sediments caused by galvanic anodes used in OWFs. However, further investigations are advisable to evaluate long-term effects over the expected lifetime of OWFs, especially with regard to the current intensification of offshore wind energy development.

1. Introduction

Renewable energy systems such as offshore wind energy play an important role to achieve the goal of sustainable energy transition and climate neutrality by 2050. The continuous rise and expansion of offshore wind power produced in offshore wind farms (OWFs) lead to a European-wide production capacity of 28 GW by the end of 2021 with 8 GW contributed by Germany (WindEurope, 2022). However, OWFs pose new anthropogenic pressures to the marine environment. Effects include, but are not limited to noise emissions, changes in ocean stratification and habitat changes (both, avoidance and attraction) (e.g. Christiansen et al., 2022; Degraer et al., 2021; Wright et al., 2020). Another aspect is possible emissions of both organic and inorganic substances from OWFs and related infrastructure (Kirchgeorg et al., 2018). Offshore structures are mainly constructed of steel, thus requiring thorough corrosion protection against harsh environmental conditions. Different corrosion protection systems are commonly applied, including galvanic anode cathodic protection, impressed current cathodic protection (ICCP), organic coatings, and corrosion allowance. Galvanic anodes dissolve over time and could therefore be a relevant source of metal emissions to the marine environment related with OWFs (Kirchgeorg et al., 2018). To protect offshore structures in seawater, Al-Zn-In-based galvanic anodes are commonly applied.

In a previous study we estimated the dissolution of at least 2164 kg of Al-Zn-In-based anode material within the planned protection period of 27 years for one offshore wind monopile (6 m diameter, 26 m submerged in water and additionally coated) (Reese et al., 2020), resulting in a continuous emission of metals into the marine environment (Kirchgeorg et al., 2018). Al-based galvanic anodes contain alloying elements like Zn (>26,200 mg kg^{-1}) and In (>143 mg kg^{-1}) which influence the physicochemical properties of the anodes. Besides, up to 25 other elements like Cd (>0.255 mg kg^{-1}), Pb (>6.7 mg kg^{-1}) or elements with low natural abundance like Ga (>78.5 mg kg^{-1}) have been found in Al-based galvanic anodes (Reese et al., 2020).

The North Sea is a very unique and dynamic marine ecosystem with highly variable geological characteristics, which is partly due to intensive sediment movements in the coastal areas, not only through natural currents (Zeiler et al., 2008) but also by anthropogenic sediment

* Corresponding author.
E-mail address: daniel.proefrock@hereon.de (D. Pröfrock).
[1] Both authors contributed equally as first author.

https://doi.org/10.1016/j.marpolbul.2023.115396
Received 8 May 2023; Received in revised form 3 August 2023; Accepted 5 August 2023
Available online 13 August 2023

relocation (Ducrotoy et al., 2000; BSH, 2016). Ocean currents in the German Bight are directed anti clockwise with water masses entering the bight from western directions and flowing north into the Skagerrak region via the Southern Jutland Current (Brückner and Mackensen, 2006). The German Bight within the North Sea is considered anthropogenically affected, which becomes particularly evident within long-term monitoring data (BSH, 2016). Mass fractions of legacy pollutants like Zn, Pb and Hg often exceed background and even effect threshold values (i.e. NOAA effect range low). In many cases elevated mass fractions are observed near the coast, which indicates possible discharges by rivers or other near-shore anthropogenic sources (BSH, 2009, 2016).

Currently, only a few studies were dedicated to the investigation of the fate of metal emissions from galvanic anodes into the marine environment. Lab-scale dissolution experiments of Zn anodes found an increase of dissolved Zn concentrations, as well as increased Zn mass fractions of marine surface sediments (Rousseau et al., 2009). A case study within the port of Le Havre (France) evaluating the dissolution of Al anodes showed that whilst anodic dissolution does not significantly increase the concentration of Al in the water, both enrichment and increased mobility of Al were evident in sediments sampled from the vicinity of the galvanic anodes (analyzed elements: Ca, Fe, K, Mg, Al and Si) (Gabelle et al., 2012). Furthermore, a five-year monitoring in the port of Calais (France) showed that the dissolution of Al anodes resulted in a higher Zn than Al enrichment of sediments. Results suggest a potential toxic effect for marine organisms with regards to the discovered Zn level, especially for confined areas with low water exchange (Caplat et al., 2020). In addition, species-specific studies showed, that the release of elements from galvanic anodes can pose effects on the species of oysters (Caplat et al., 2012; Mottin et al., 2012; Golding et al., 2015; Levallois et al., 2022), blue mussels (Mao et al., 2011; Golding et al., 2015), sea urchins (Caplat et al., 2010; Golding et al., 2015), amphipods (Bell et al., 2020), diatoms (Golding et al., 2015; Bell et al., 2020) and bacteria (Bell et al., 2020) and that in combination with other stressors such as noise the effect of a metal exposure is enhanced for biota such as lobsters (Stenton et al., 2022). In contrast, another recent study in La Rochelle (France) concludes that effects on the health of scallops cannot clearly be appointed to be caused by galvanic anodes (Barbarin et al., 2023). Moreover, the impact of climate change itself could increase metal release and the mortality of biota inhabiting wind farms due to higher water temperature and lower pH (Voet et al., 2022).

Recently, Wang et al. (2023) applied geo-accumulation index, contamination factor and pollution load index to sediments taken in the Putidao OWF (China). First hints on heavy metal pollution (Cu, Pb, Zn, Cr and Cd) caused by OWFs were found (Wang et al., 2018). Moreover, the authors suggest future long-term monitoring for a sound assessment of the impact of offshore wind farms on the marine environment.

Therefore, the analysis of elemental mass fractions in sediments is one important aspect for the assessment of long-term or emerging contamination of aquatic systems potentially caused by the dissolution of galvanic anodes in connection with the ongoing large-scale development of renewable energy production worldwide. We previously suggested a multi-tracer approach for the investigation of OWF-induced emissions from galvanic anodes consisting of the elements Cd and Pb, as ecotoxicologically relevant legacy pollutants, the previously discussed main components Al and Zn and the technology-critical elements (TCEs) In and Ga. Moreover, the application of Pb isotope ratios and element ratios was suggested (Reese et al., 2020). Despite an increasing scientific interest in and usage of the elements Ga and In, these elements still show a lack of knowledge regarding their (eco)toxicity, their respective environmental speciation and potential impact on the (marine) environment (Filella and Rodriguez-Murillo, 2017; Romero-Freire et al., 2019).

In addition to elemental analysis metal stable isotope ratios have been shown to be a powerful tool for environmental source and process tracing (Wiederhold, 2015). The isotope amount ratio $n(^{87}Sr)/n(^{86}Sr)$ can be used as a measure for the age and/or type of rocks and sediments (Capo et al., 1998), as the relative abundance of the radiogenic isotope ^{87}Sr increases by the radioactive β^--decay of ^{87}Rb ($t_{1/2} = 4.88 \cdot 10^{10}$ a) (Brand et al., 2014; de Laeter et al., 2003). Typically, finer sediment fractions are more radiogenic than sandy sediments, due to an enrichment of Rb-rich minerals in the fine sediments (Bayon et al., 2021). Several studies have investigated Sr isotope ratios for provenancing and characterization of sediments, e.g. (Andrews et al., 2016, Reese et al., 2019, Bayon et al., 2021, Deng et al., 2021).

This study provides a first baseline dataset regarding the spatial and temporal variation of galvanic anode tracer elements of German North Sea sediments inside and within the surroundings of different OWFs over the course of seven years. A multi-element and Sr-isotope tracer approach was applied to assess possible inputs of metal contaminants originating from OWFs and to differentiate from other sources. This work can be used as the basis of future studies on potential mid- and long-term chemical emissions and environmental effects related to the ongoing development of renewable offshore energy production.

2. Material and methods

2.1. Reagents and materials

All preparatory laboratory work was performed in a class 10,000 or class 1000 clean room. Type I reagent-grade water (18.2 MΩ cm) was obtained from a Milli-Q Integral water purification system equipped with a QPod-Element polishing system (Merck-Millipore, Darmstadt, Germany). Analytical grade HNO_3 (w = 65 %, Fisher Scientific, Schwerte, Germany) and analytical grade HCl (w = 30 %, Carl Roth, Karlsruhe, Germany) were further purified either by double sub-boiling in perfluoralkoxy-polymer (PFA)-subboling stills (DST-4000 & DST-1000, Savillex, Minnesota, USA) or by double sub-boiling using a cascade of two quartz stills (AHF Analysentechnik, Tübingen, Germany) operated under clean room conditions. HBF_4 (w = 38 %, Chem-Lab, Zedelgem, Belgium) was used in ultra-pure quality for sample digestion without any further purification.

External calibration standard solutions for quantification (all traceable to NIST standards) were prepared from custom-made multi-element standards of different composition (Inorganic Ventures, Christiansburg, USA).

The reference marine sediments GBW 07313 (National Research Centre for Certified Reference Materials, Beijing, China) and the reference stream sediment GBW 07311 (National Research Centre for Certified Reference Materials) were used for method validation.

2.2. Sampling

A total of 215 sediment samples were obtained from OWFs in the German North Sea during six sampling campaigns with the research vessels Atair (Federal Maritime and Hydrographic Agency, BSH) in 2018, 2019, 2021 and 2022 and the Ludwig Prandtl (Hereon) in 2016 and 2020. Due to logistical challenges and weather conditions not all sampling stations were sampled in every year. Samples were taken via a box-corer in and around selected OWFs. Due to safety reasons and legal restrictions it was not possible to obtain samples directly next to the foundations or in certain corridors due to the presence of the OWF underwater power cables. The top layer (upper 5 cm) of three or more individual box-cores from the same sampling station were combined, homogenized and stored at −20 °C until further analysis. A list of all samples including GPS coordinates can be found in the electronic supplementary material (ESM) Table A4. A map of all sampling locations for the six cruises is shown in Fig. 1. Table 1 gives an overview over the number of samples taken in the respective OWF areas per year.

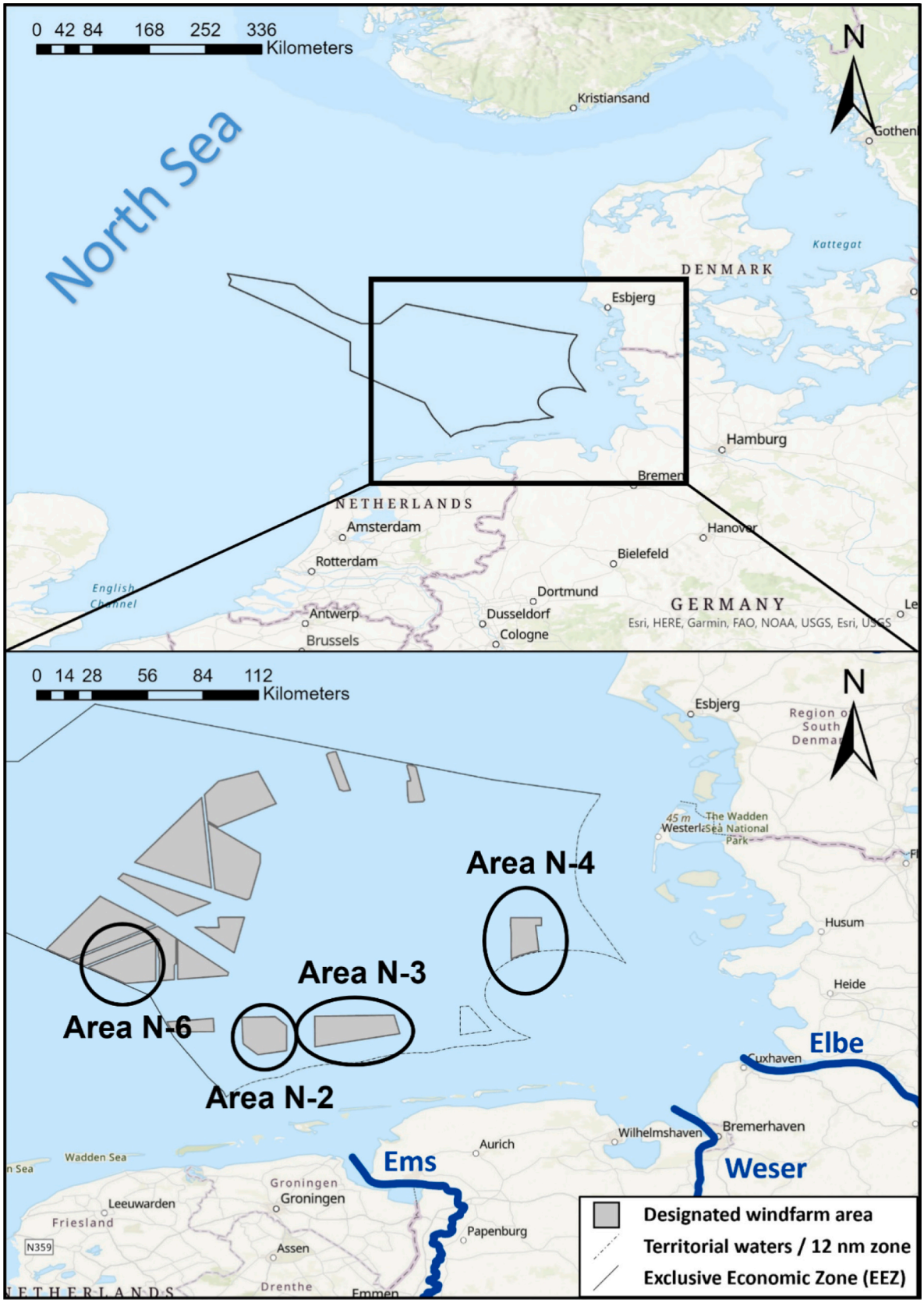

Fig. 1. Top: Overview of the North Sea. Bottom: Sampling areas in and around OWFs in the German Bight (grey areas) within the exclusive economic zone (EEZ). The investigated areas are labeled according to the site development plan for the German North Sea and Baltic Sea (BSH, 2023). Tributaries of the German Bight (Weser, Ems and Elbe) are highlighted in blue. (For interpretation of the references to colour in this figure legend, the reader is referred to the web version of this article.)

Table 1
Overview of sample stations (*n*) per campaign and area.

	Area N-2	Area N-3	Area N-4	Area N-6
LP20160725 (2016)	–	–	18	–
AT261 (2018)	14	20	18	–
AT275 (2019)	15	22	33	10
LP2020629 (2020)	–	3	16	–
AT004 (2021)	2	3	10	8
AT010 (2022)	3	3	11	1

2.3. Sample preparation

The frozen sediment samples were freeze-dried (Christ Gefriertrocknungsanlagen, Osterode, Germany) and wet-sieved over a cascade of sieves (Atechnik, Leinburg, Germany). The <20 μm fraction of the sediments was obtained by continuous flow centrifugation (Contifuge Stratos, Thermo Scientific, Waltham, USA) in conjunction with a titanium rotor (Continous Flow Rotor 3049, Thermo Scientific) after passing the last sieve with a mesh size of 20 μm.

Dried fine-grain sediment aliquots of 50 mg were digested in triplicates with 5 mL HNO_3, 2 mL HCl and 1 mL HBF_4 for 300 min at 180 °C either with a MARS Xpress or a MARS 6 microwave (CEM Corp., Kamp Lintfort, Germany) in 55 mL pre-cleaned TFM digestion vessels following the protocol described by Zimmermann et al. (2020). The marine sediment reference materials GBW 07311 and GBW 07313 were treated similarly and digested in duplicates per digestion batch (12 samples in triplicates). The reference material was quantitatively digested by the presented digestion method resulting in clear, particle free digests.

For the analysis of Sr isotope ratios aliquots of the digested sediment were transferred to a pre-cleaned 50 mL DigiTUBE (SCP Science, Quebec, Canada), evaporated to dryness at 75 °C and re-dissolved in 1 mL of 2 mol L^{-1} HNO_3. Matrix separation was performed following an automated separation procedure using the fully automated sample preparation system prepFAST-MC® (Elemental Scientific, Omaha, USA). A self-packed column with 3 mL bed volume (ESI part. no. CF-3000) packed with DGA Resin (DN-B100-S, TrisKem International, Bruz, France) was utilized. The separation protocol is based on Retzmann et al. (2017) and Zimmermann et al. (2019b). All steps of the separation procedure can also be found in ESM Table A1.

2.4. Instrumental analysis

2.4.1. Grain size analysis

The grain size distribution of each sediment sample was determined by laser diffraction (Analysette 22 NanoTec, Fritsch, Idar-Oberstein, Germany).

2.4.2. Multi-element analysis

Determination of elemental mass fractions in the sediment digests was performed using an inductively coupled plasma tandem mass spectrometer (ICP-MS/MS) (Agilent 8800, Agilent Technologies, Tokyo, Japan) coupled to an ESI SC-4 DX FAST autosampler (Elemental Scientific, Omaha, Nebraska, USA) (Pröfrock and Prange, 2012). A list of measured isotopes and their detection modes can be found in ESM Table A2. A detailed description of all ICP-MS/MS operating parameters and used cell gas modes can be found in ESM Table A3. The instrument was tuned daily using a tune solution containing Li, Co Y, Ce and Tl at a concentration of 10 μg L^{-1}. Quantification was performed by external calibration covering a concentration range from 0 μg L^{-1} to 10,000 μg L^{-1} for Mg, Al, K, Ca, Ti, Fe, Mn, Ba and P and 0 μg L^{-1} to 100 μg L^{-1} for all other analytes. Solutions and blanks were prepared on a daily basis from custom made multi-element standards (Inorganic Ventures, Christiansburg, USA). Wash blanks were measured after each sample triplicate to monitor and avoid potential carry-over effects.

2.4.3. Isotopic analysis

The analysis of Sr isotope ratios was performed according to the method described by Retzmann et al. (2017). A multi collector inductively coupled plasma mass spectrometer (MC ICP-MS) (Nu Plasma II, Nu Instruments Ltd., Wrexham, UK) was used for the measurement. The instrument was equipped with an APEX omega membrane desolvation system (Elemental Scientific, Omaha, Nebraska, USA) in combination with a PFA micro flow nebulizer (Elemental Scientific, Omaha, Nebraska, USA) as sample introduction system. All measurements were performed in static measurement mode with low mass resolution. Data collection was accomplished over a period of 600 s with an integration time of 10 s, resulting in 60 measurements per sample. Sr concentrations of samples and bracketing standards (NIST SRM 987) were matched within ±10 % in terms of the obtained signal intensities prior to analysis. Sr fractions and the corresponding isotopic standard were doped with Zr (Merck-Millipore) as internal standard for correction of instrumental isotopic fractionation (IIF) (Horsky et al., 2016).

2.5. Data evaluation and presentation

2.5.1. Multi-element analysis

Multi-element data were processed using MassHunter version 4.4 or higher (Agilent Technologies, Tokyo, Japan) and a custom written Excel© spreadsheet. The isobaric interference of ^{115}Sn on ^{115}In was corrected for by peak stripping as implemented in MassHunter using the signal of ^{118}Sn and the isotopic abundances provided by IUPAC's Commission on Isotopic Abundances and Atomic Weights (de Laeter et al., 2003). The Limits of detection (*LOD*) and Limits of quantification (*LOQ*) were calculated according to DIN 32645 (2008) and DIN ISO 11843-2 (2006). Combined uncertainties were estimated using a *Kragten* spreadsheet approach (Kragten, 1994) taking into account reproducibility, repeatability and measurement precision for each sample. The significant number of digits of elemental mass fractions are given according to GUM and EURACHEM guidelines, whereby the uncertainty determines the significant number of digits to be presented with the value (EURACHEM/CITAC, 2012).

2.5.2. Isotopic analysis

The IIF was corrected for by following an internal inter-elemental approach combining standard sample bracketing and external calibration to account for time dependent and matrix dependent IIF variation between the samples as described elsewhere (Horsky et al., 2016; Retzmann et al., 2017). Isobaric interferences of residual $^{87}Rb^{+}$ on $^{87}Sr^{+}$ were subtracted via peak stripping. The detailed calculation approach for Sr isotope ratio analysis and data processing including all equations and constants as well as reference values used for interference and IIF correction are given elsewhere (Retzmann et al., 2017).

Total combined uncertainty budgets were determined considering sample inhomogeneity, precision of the isotope ratio measurement for samples and standards and within-run repeatability of the measured isotope ratio in the bracketing standards as proxy for instrument stability (Horsky et al., 2016; Reese et al., 2019).

2.5.3. Data assessment criteria

In order to obtain comparable and standardized elemental mass fractions in sediments, different normalization approaches are commonly applied. Isolation of the fine grain fraction by (wet-) sieving (size fraction <20 μm or <63 μm) can be regarded as a physical normalization reducing differences in the granulometric composition. The wet-sieving was performed in a closed set-up using 1 L of MilliQ water. Leaching of analytes into the water used for sieving is negligible (between 5×10^{-5} % and 5×10^{-9} % for all analytes) (Nham, 2017). Coarser particles, which usually do not bind anthropogenic contaminants and would therefore dilute their elemental mass fractions, are removed from the sample (Ackermann et al., 1983). To ensure comparability with the long-term reports of the BSH on the assessment of metal

pollutants in North Sea sediments only the <20 μm size fraction of the sediment was analyzed. Current monitoring reports include information on the six elements Cd, Cu, Hg, Ni, Pb and Zn (BSH, 2016).

Measured elemental mass fractions of the OWF areas were compared to three types of benchmark mass fractions: geogenic background concentrations, recent North Sea sediment data and (no-) effect concentrations, as summarized in Table 2. Geogenic background concentrations (BSH BC), derived from the fine grain fraction (grain size <20 μm) of older, presumably largely unpolluted sediment core samples from the German Exclusive Economic Zone (EEZ), was utilized for Cd, Pb and Zn (BSH, 2016). Recent North Sea sediment data is available for the elements Cd, Pb and Zn from the BSH monitoring program for the years 2008–2011 (BSH, 2016). For Ga and In, no BSH BC nor comparable region-specific background is currently available. Therefore, Ga and In data of this study are compared to the abundances in the upper continental crust (UCC) according to Rudnick and Gao (Rudnick and Gao, 2003), as well as Ga and In data for recent North Sea sediments published by Klein et al. derived from the retrospective analysis of sediments sampled between 2010 and 2020 (Klein et al., 2022a). The US National Oceanic and Atmospheric Administration (NOAA) derived Effect Range Low values (NOAA ERLs) for Cd, Pb and Zn as a numerical quality criterion and are derived from biological effect data from the "NOAA Sediment Quality Guidelines". In the OSPAR region the NOAA ERLs are applied as criteria to assess the environmental status of metal concentrations. It represents a pollutant concentration below which only 10 % of the systems show effects (Macdonald et al., 1996). No NOAA ERLs are available for In and Ga. However, the European Chemicals Agency ECHA derived a Predicted No-Effect Concentration (PNEC) for In in (marine) sediments. For Ga no such concentration was defined yet.

2.5.4. Data presentation

The measured sediment data is presented in box plots, indicating the median of the respective data volume (line, P50) with 98 % confidence interval, the interquartile range (P25 – P75) limited by the lower and upper limit of the box and the extreme values of the respective data series. Measured values with a distance of 1.5 interquartile ranges that exceed the interquartile limits are identified by dots as outliers. Numbers in the box plots indicate minimum and maximum values excluding outliers.

2.5.5. Distribution maps

Geographical maps showing selected parameters were created using ArcGIS® software by Esri. ArcGIS® and ArcMap™ are the intellectual property of Esri and are used herein under license.

Table 2
Criteria for evaluating the metal content in marine sediment. Geogenic background values (BSH BC (BSH, 2016) or UCC (Rudnick and Gao, 2003)), recent elemental mass fraction ranges in the German EEZ (<20 μm) ((BSH, 2016; Klein et al., 2022a)) and ecological (no-effect) evaluation criteria (NOAA ERL (Macdonald et al., 1996) or PNEC (ECHA, 2020)).

	Zn/mg kg^{-1}	Ga/mg kg^{-1}	Cd/mg kg^{-1}	In/mg kg^{-1}	Pb/mg kg^{-1}
Geogenic background	81–116[a]	17.5 ± 0.7[c]	0.08–0.26[a]	0.056 ± 0.008[c]	12–38[a]
Recent North Sea sediment	158-864[a]	14-23[d]	0.15–0.87[a]	0.073-0.237[d]	66-182[a]
No-effect concentration	150[b]	–	1.2[b]	5051[e]	46.7[b]

[a] (BSH, 2016).
[b] (Macdonald et al., 1996).
[c] (Rudnick and Gao, 2003).
[d] (Klein et al., 2022a).
[e] (ECHA, 2020).

3. Results

3.1. Elemental mass fractions

In total, elemental mass fractions of 55 elements were measured in 215 North Sea sediment samples (<20 μm size fraction). The complete data set for all measured elements and grain size distributions can be found in ESM Tables A4 and A5. The following section describes the distribution of selected elements (Cd, Ga, In, Pb, Zn) in samples obtained during the six sampling campaigns. The selection of the presented elements is based on work by Reese et al. (2020) who suggested Al, Cd, Ga, In, Pb, Zn as element tracers for potential emissions from galvanic anodes applied for corrosion protection of OWFs. Although Al is the main component of galvanic anodes, it is not further discussed individually, since due to its high natural background in North Sea sediments and a naturally high variability (in 2010/2011 between 6.1 % and 7.7 % in <20 μm in the German Bight, BSH, 2016), it is currently not possible to differentiate individual sources (BSH, 2016; Reese et al., 2020). Distribution maps for the selected five elements can be found in the ESM Figs. A1, A4, A7, A10 and A13.

3.1.1. Cadmium (Cd)

The mass fractions of Cd (see Fig. 2A, the distribution map in ESM Fig. A1, a detailed distribution map for area N-4 in ESM Fig. A2 and a high-resolution boxplot in ESM Fig. A3) range between 88 μg kg^{-1} ± 44 μg kg^{-1} and 1150 μg kg^{-1} ± 130 μg kg^{-1}. Even though the measured Cd mass fractions (except area N-6 (2019)) exceed the BSH BC (80 μg kg^{-1} to 260 μg kg^{-1}), most samples are within the known mass fraction range of German North Sea sediments (150 μg kg^{-1} to 870 μg kg^{-1} (BSH, 2016)) and are below the NOAA ERL of 1200 μg kg^{-1} (Macdonald et al., 1996). However, area N-2 (2021), area N-3 (2022) and area N-4 (2022) feature values close to the NOAA ERL, even though their median values are within the mass fraction range of North Sea sediments. Indeed, this can only be observed for a very limited number of samples.

3.1.2. Lead (Pb)

The Pb mass fractions (see Fig. 2B, the distribution map in ESM Fig. A4, a detailed distribution map for area N-4 in ESM Fig. A5 and a high-resolution boxplot in ESM Fig. A6) range between 47 mg kg^{-1} ± 1 mg kg^{-1} and 420 mg kg^{-1} ± 40 mg kg^{-1}. Measured mass fractions are higher than the BSH BC of 12 mg kg^{-1} to 38 mg kg^{-1} and higher than the NOAA ERL of 46.7 mg kg^{-1} (BSH, 2016; Macdonald et al., 1996). However, median mass fractions of most areas are within the known variability of German North Sea sediments ranging from 66 mg kg^{-1} to 182 mg kg^{-1} (BSH, 2016). Slightly higher median mass fractions are found for area N-4 in 2016 and 2019 (median: 199 mg kg^{-1} and 194 mg kg^{-1}, respectively). Overall, area N-2 (2018 and 2019), area N-3 (2019) and area N-4 (2016–2020) show values above the variability of North Sea sediments (BSH, 2016). Latest mass fractions (samples from 2021 and 2022) are within the variability of North Sea sediments for all areas, indicating a steady pollution load for areas N-2 and N-3 and suggesting slightly decreasing mass fractions for areas N-4 and N-6.

3.1.3. Zinc (Zn)

The Zn mass fractions (see Fig. 2C, the distribution map in ESM Fig. A7, a detailed distribution map for area N-4 in ESM Fig. A8 and a high-resolution boxplot in ESM Fig. A9) range from 108 mg kg^{-1} ± 1 mg kg^{-1} to 820 mg kg^{-1} ± 36 mg kg^{-1}. Almost all samples exceed the BSH BC of 81 mg kg^{-1} to 116 mg kg^{-1} and the NOAA ERL of 150 mg kg^{-1} (BSH, 2016; Macdonald et al., 1996). Samples from area N-6 are slightly above the BSH BC range and slightly below the NOAA ERL. Nevertheless, median mass fractions of all other areas are within the known variability of German North Sea sediments ranging between 158 mg kg^{-1} and 864 mg kg^{-1} (BSH, 2016). Area N-2 and area N-3 feature significantly lower Zn mass fractions and a lower variability than area N-4.

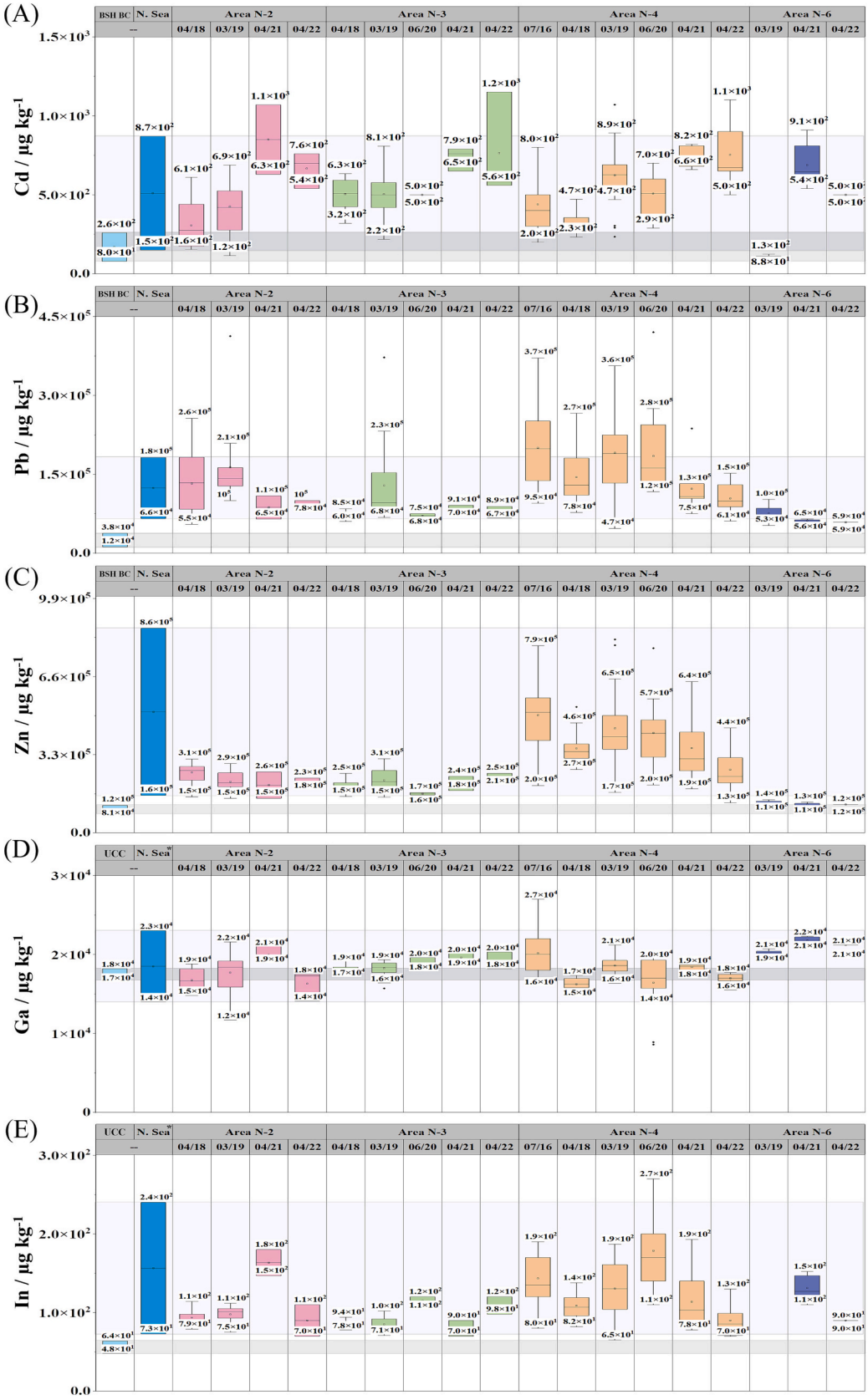

Fig. 2. Metal mass fractions in North Sea (N. Sea) sediments in and around OWFs of the German Bight for (A) Cd, (B) Pb, (C) Zn, (D) Ga and (E) In. The samples are grouped according to the official designation of the site development plan for the German North Sea and Baltic Sea by the BSH (2023). Reference values are given as UCC = crustal abundance (Rudnick and Gao, 2003); N. Sea* = mass fraction range of North Sea sediments between 2010 and 2020 (Klein et al., 2022a), N. Sea = mass fraction range of North Sea sediments between 2008 and 2011 (BSH, 2016) and BSH BC = BSH background value (BSH, 2016). *The following elemental mass fractions are within Fig. 2 as outliers, but covered by the labels of the whiskers: Pb: Area-N6, 04/21, 7.5 × 10^5 µg kg^{-1}; Zn: Area N-6, 04/21, 1.4 × 10^5 µg kg^{-1}; Ga: Area N-4, 04/21, 2.0 × 10 µg kg^{-1} and In: Area N-3, 04/18, 9.7 × 10^2 µg kg^{-1}.

3.1.4. Gallium (Ga)

The Ga mass fractions (see Fig. 2D, the distribution map in ESM Fig. A10, a detailed distribution map for area N-4 in ESM Fig. A11 and a high-resolution boxplot in ESM Fig. A12) range between 8.6 mg kg^{-1} ± 0.5 mg kg^{-1} and 27 mg kg^{-1} ± 14 mg kg^{-1}. The majority of the analyzed samples feature Ga mass fractions within the range of North Sea sediments as published by Klein et al. (2022a) (14 mg kg^{-1} ± 1 mg kg^{-1} to 23 mg kg^{-1} ± 5 mg kg^{-1}), which is close to the crustal abundance of 17.5 mg kg^{-1} ± 0.7 mg kg^{-1} (Rudnick and Gao, 2003). Slightly higher mass fractions are found in area N-4 (2016) for two samples with mass fractions of 25 mg kg^{-1} ± 1 mg kg^{-1} and 27 mg kg^{-1} ± 14 mg kg^{-1}.

3.1.5. Indium (In)

The In mass fractions (see Fig. 2E the distribution map in ESM Fig. A13, and a high-resolution boxplot in ESM Fig. A14) range between 65 µg kg^{-1} ± 9 µg kg^{-1} and 270 µg kg^{-1} ± 30 µg kg^{-1}. In mass fractions of all samples are significantly higher than the crustal abundance of 56 µg kg^{-1} ± 8 µg kg^{-1} (Rudnick and Gao, 2003). However, median mass fractions of most areas are within the variability of North Sea sediments of 73 µg kg^{-1} ± 4 µg kg^{-1} to 237 µg kg^{-1} ± 13 µg kg^{-1} as published by Klein et al. (2022a), except for area N-3 (2018, 2019 and 2021) showing median mass fractions slightly below the reference range. Area N-2 shows increased mass fractions in 2021 compared to previous years, but mass fractions from 2022 are in the range of 2018 and 2019 again. Area N-2 and N-3 show lower variability than area N-4. All mass fractions fall below the PNEC of 5051 mg kg^{-1} (ECHA, 2020) by far.

3.2. Sr isotope ratios

Isotope amount ratios of Sr were analyzed in the sediment samples taken in 2018 and 2019. The data is given in ESM Table A6 and distribution maps of the isotope ratio $n(^{87}Sr)/n(^{86}Sr)$[2] can be found in ESM Fig. A15. For both years $n(^{87}Sr)/n(^{86}Sr)$ ranged between 0.71247 ± 0.00014 and 0.71767 ± 0.00014. Fig. 3A shows $n(^{87}Sr)/n(^{86}Sr)$ plotted against the inverse Sr mass fraction. The OWF area N-4 north of Heligoland features significantly heavier isotope ratios and higher Sr mass fractions than the OWF areas N-2, N-3 and N-6 in the western area of the German Bight. The isotope-amount ratio $n(^{87}Sr)/n(^{86}Sr)$ can be used as a measure for the age and/or type of rocks and sediments as well as their origin: The ratio $n(^{87}Sr)/n(^{86}Sr)$ varies as the relative abundance of the radiogenic isotope ^{87}Sr increases by the radioactive decay of ^{87}Rb. Therefore, $n(^{87}Sr)/n(^{86}Sr)$ depends on the geological age and initial amount of Rb in the source materials and therefore its origin. Moreover, Sr isotope-amount ratios may depend on the grain size of the analyzed sediment sample. Finer sediment fractions are more radiogenic than sandy sediments, due to an enrichment of Rb-rich minerals in the grain size fraction (Bayon et al., 2021). As can be seen in Fig. 3A $n(^{87}Sr)/n(^{86}Sr)$ plotted against the inverse Sr mass fractions results in samples grouped along a linear regression, thus indicating the mixing of at least two different sediment types with different geological origin. Sediment samples with higher isotope amount ratios are in good accordance with literature data for sediments from the Elbe estuary (Reese et al., 2019.) and the lower Weser (Deng et al., 2021) (both measured in the <63 µm size fraction), thus, suggesting a significant proportion of sediments originating from the North Sea's tributaries. However, future analysis of further endmembers are required for an in-depth source tracing.

Together with the share of the <20 µm grain size fraction (Fig. 3B) the four areas feature different characteristics: Sediments from area N-2 have generally low amounts of the fine grain size fraction (<8 %) and low $n(^{87}Sr)/n(^{86}Sr)$ values (0.71247 ± 0.00014 to 0.71516 ± 0.00017). Sediments of area N-3 feature a similar range of $n(^{87}Sr)/n(^{86}Sr)$ values (0.71273 ± 0.00015 to 0.7150 ± 0.0004) with higher amounts of the <20 µm grain size fraction (4 % to 15 %). Sediments of area N-4 show significantly heavier isotope ratios (0.71421 ± 0.00015 to 0.71767 ± 0.00014) together with a broad variation in the <20 µm grain size fraction (0.6 % to 19 %). The highest amounts of the <20 µm grain size fraction can be found in the sediments of area N-6 (7 % to 22 %) which are accompanied by a narrow range in $n(^{87}Sr)/n(^{86}Sr)$ (0.71462 ± 0.00015 to 0.71484 ± 0.00015).

4. Discussion

The following discussion of selected elements is based on work by Reese et al. (2020) who suggested Cd, Ga, In, Pb and Zn as the most promising tracers for potential emissions from galvanic anodes. In general, the dataset demonstrated a high variability likely due to the complex hydrographic dynamics and sediment movement in the North Sea as well as different further sources (e.g. riverine inputs) and natural variation for metals. The data is provided in ESM Table A5 together with the mass fractions of 50 other elements analyzed in the samples from the different sampling locations.

4.1. Temporal variation of elemental mass fractions

The tracers Cd, Ga, In, Pb and Zn do not indicate a clear accumulation in the investigated areas, due to the short time series and high variability of the data. However, here we will discuss some features observed in the data.

Median Cd mass fractions for areas N-2, N-3 and N-4 were the highest for samples taken 2021 and 2022 compared to previous years sampled within this study, suggesting either increased Cd inputs or remobilization of older, contaminated sediments. Yet, all Cd values measured in the present study are below the NOAA ERL, therefore, no significant effects on the marine environment caused by Cd is to be expected at the current stage. The majority of the sampled OWFs were built between 2013 and 2017. Each area consists of 150 to 200 offshore wind turbines. Therefore, considering five years and 150 offshore wind turbines, a release of 14 g to 420 g of Cd by galvanic anodes can be estimated (Reese et al., 2020). Consequently, the potential increase of Cd mass fractions is unlikely solely caused by galvanic anodes of OWFs. The increase might be related to sources like remobilization of older sediments (Carpenter et al., 2016; Forster, 2018), inputs by river discharges, e.g. the Elbe, Rhine and Weser rivers (Deng et al., 2021; Klein et al., 2022b; Reese et al., 2019) or dissolution of Zn galvanic anodes used for corrosion protection of ship hulls (OSPAR, 2009). These anodes contain 100-times more Cd than Al-based anodes, with Cd being the third most abundant metal after Zn and Al (Reese et al., 2020).

Similar to Cd, sediment samples from area N-2 (2018, 2019), area N-3 (2019) and area N-4 (2016–2020) feature Pb mass fractions above the reported variability of North Sea sediments. Indeed, median mass fractions tend to be lower and within the expected range of North Sea sediments for samples taken in recent years (2021 and 2022) for all areas, thus, rather indicating decreasing Pb mass fractions. Nevertheless, mass fractions of Pb in the analyzed samples exceed the NOAA ERL, like in most parts of the German Bight (OSPAR, 2010; von der Au et al., 2022). For Al-based anodes a release of 390 g to 580 g of Pb can be estimated for an OWF area of 150 monopiles within five years (Reese et al., 2020). As Pb is a particle active element, inputs of dissolved Pb will quickly adsorb onto suspended particulate matter and thus accumulate in the sediment or might be dispersed or transported also over larger distances or even will find its way into the marine food chain via filter feeding organisms (Kremling et al., 1999). Pb is introduced into the marine environment by a wide variety of other mostly anthropogenic sources, such as industrial applications (Boyle et al., 2014) or combustion processes of fossil fuels (Komarek et al., 2008; Larsen et al., 2012). Also a remobilization from

[2] IUPAC-recommended notation for SI-traceable isotope-amount ratios $r = n(^{i}E)/n(^{j}E)$, with the amount of substance n, and the isotopes ^{i}E and ^{j}E of the element E. The notation $^{i}E/^{j}E$ (e.g. $^{87}Sr/^{86}Sr$) is commonly used interchangeably, even though lacking information on the type of quantity (microscopic vs. macroscopic) (see also Coplen, 2011).

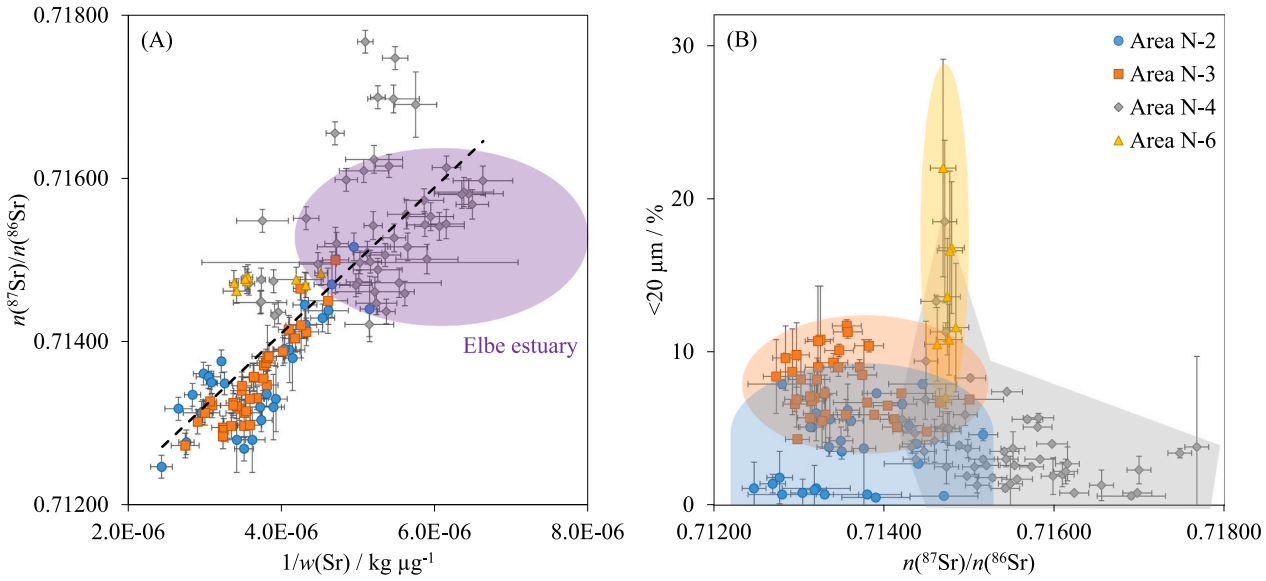

Fig. 3. (A) Isotope ratio $n(^{87}Sr)/n(^{86}Sr)$ plotted against the inverse Sr mass fraction. The purple area corresponds to data from Elbe estuary sediments (Reese et al., 2019). (B) Share of the <20 µm grain size fraction in the sediment samples plotted against the isotope ratio $n(^{87}Sr)/n(^{86}Sr)$. The data points are grouped into the respective OWF areas. Error bars correspond to expanded uncertainties $U(k = 2)$ for isotope ratios and inverse mass fractions and to standard deviation ($n = 3$) for the grain size fraction. (For interpretation of the references to colour in this figure legend, the reader is referred to the web version of this article.)

older sediment reservoirs (legacy pollution) due to changing current conditions in the direct surrounding of the individual foundations might be possible.

Temporal variations of the measured Zn mass fraction are very small for the areas N-2, N-3 and N-6 over the studied timeframe indicating no increase of mass fractions of Zn in sediments within the vicinity of OWFs. The largest variations can be observed for area N-4. Indeed, Zn mass fractions in most of the analyzed sediment samples are above the NOAA ERL indicating potential effects on the marine environment. Some marine species are reported to be very sensitive to increased Zn concentrations in the water phase (Peganova and Eder, 2004), including changes in growth of marine cyanobacteria (Sarker et al., 2021). The continuous release of anode material has the potential to further increase environmental concentrations. As Zn is the second most abundant element in Al based galvanic anodes a release of 1600 kg to 3600 kg Zn in each OWF area can be conservatively estimated, considering five years and 150 offshore wind turbines per OWF area. Zn is a so-called recycled or nutrient type element in the context of seawater, hence, long residence times in seawater (10^3–10^5 years) are typical (Kremling et al., 1999) and enrichments are more likely to be observed in the water phase. Long-term monitoring data by the BSH (2016) shows that elevated mass fractions of Zn in the German North Sea were observed even before the construction of the first OWFs in 2012 (BSH, 2016), likely due to other sources such as shipping (OSPAR, 2009), river discharges (Reese et al., 2019; Zimmermann et al., 2019a), or, especially for OWF area N-4 located north of Heligoland, historical dumping of dilute acid waste until 1989 (BSH, 1991; Pickaver, 1982). Due to the very complex source situation and the long residence time of Zn in seawater, the current Zn pollution in the OWF areas under consideration cannot be clearly attributed to new emissions of OWFs.

In contrast to the legacy pollutants Cd, Zn and Pb, the TCEs Ga and In can be considered emerging contaminants with almost no currently known anthropogenic sources into the marine environment (Romero-Freire et al., 2019). Both elements are added to galvanic anode alloys to avoid passivation of the Al surface and hence promote the dissolution of the anode instead of the steel structure. For a five year protection of one OWF area of 150 coated offshore wind turbines the release of 5 kg to 8 kg Ga and 9 kg to 14 kg In can be estimated (Reese et al., 2020). Like Pb, Ga and In are assumed to be particle-active elements in seawater, meaning that these elements are transported over the particulate matter into the sediments with short resident times in seawater (Klein et al., 2022b; Kremling et al., 1999; Romero-Freire et al., 2019). All median mass fractions of Ga are within the range of North Sea sediments as published by Klein et al. (2022a). Median mass fractions are higher in the areas N-2 and N-6 for 2021, but decrease again in 2022. The highest inter-year variability for Ga can be observed for area N-4. Very similar observations can be made for In: All In median mass fractions are within the range of North Sea Sediments as published by Klein et al. (2022a). The highest inter-year variability for In can be observed for area N-4 with the highest values in 2020, decreasing in 2021 and 2022. Similarly, area N-2 features highest mass fractions in 2021, but decreased to mass fractions similar to 2018 and 2019 in 2022. This might be also caused by the high known sea bed dynamics in the German Bight (Zeiler et al., 2008), which results also in the spatial transport and dispersion of fresh pollutant-loaded sediments.

4.2. *Spatial distribution of Indium mass fractions*

The spatial distribution of elemental mass fractions in and around OWFs area N-4 will be discussed in detail in this chapter, as it features the highest sample density over the longest time period during this study, combined with the highest intra-year variability for the tracer elements. As In is the most promising tracer for anode emissions, the spatial distribution is discussed for In, as shown in Fig. 4. Corresponding maps for all other tracer elements (Cd, Pb, Zn, Ga) can be found in ESM Figs. A2, A5, A8, A11. As can be seen from the first sampling campaign in 2016 (Fig. 4A) the distribution of In mass fractions seems to follow a North-South gradient with higher elemental mass fractions in the northern region (140 µg kg^{-1} ± 30 µg kg^{-1} to 190 µg kg^{-1} ± 40 µg kg^{-1}) compared to the southern region (80 µg kg^{-1} ± 20 µg kg^{-1} to 130 µg kg^{-1} ± 10 µg kg^{-1}). However, this was not necessarily true for all five following sampling campaigns in 2018, 2019, 2020, 2021 and 2022 (Fig. 4B–F). Recent literature indicates an increase of metal concentration with decreasing distance to the wind farm center (Wang et al., 2023). In our study the highest In mass fractions occurred in 2020 (marked dark red in Fig. 4D). High In mass fractions (light red) were found in 2016, 2019, 2020 and 2021, again outside or at the edge of the OWF, except for 2019. Indium mass fractions in 2019 (Fig. 4C) show a

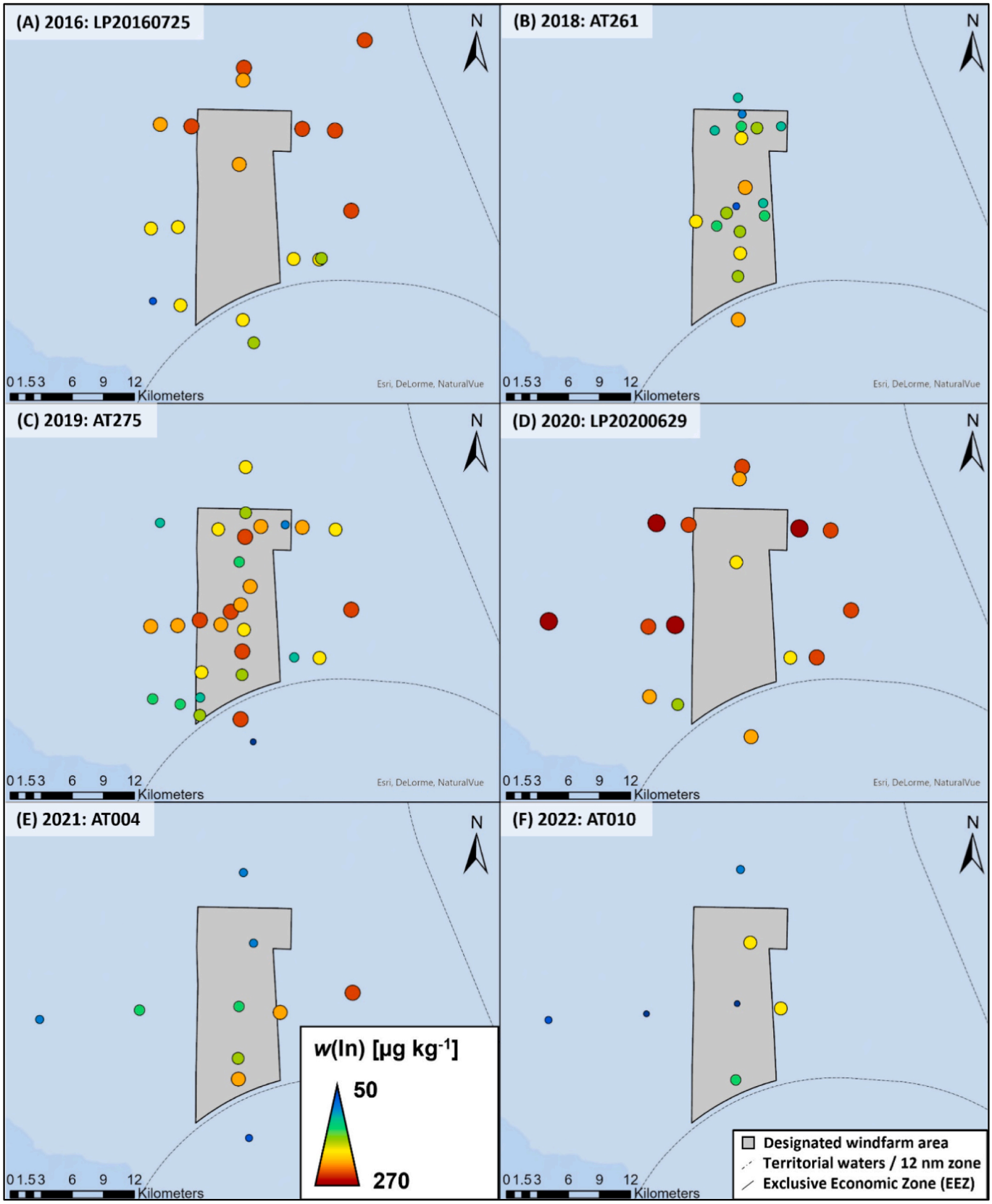

Fig. 4. Spatial distribution of In mass fractions in North Sea sediments in and around OWF area N-4 in A) 2016, B) 2018, C) 2019, D) 2020, E) 2021 and F) 2022. The investigated area is labeled according to the official designation of the site development plan for the German North Sea and Baltic Sea by the BSH (2023).

higher density of high mass fractions within the OWF compared to outside or at the edge of the OWF. This would support the results of Wang et al. (2023) if these values are considered independently from the other campaigns. However, taking the sampling campaigns in 2018, 2021 and 2022 (Fig. 4B, E, F) into account, this observation cannot be confirmed. For samples taken in 2018 with a high sample density within the OWF, a quite homogeneous distribution of In mass fractions and overall significantly lower mass fractions than 2019 were observed. Nonetheless an enrichment of In from 2018 to 2019/2020 seems unlikely, since the latest campaigns (2021 and 2022 Fig. 4E, F) show In mass fractions comparable to 2018 and below. Overall the high spatial as well as temporal variations of In elemental mass fractions emphasize the complexity of a sound source attribution of possible metal emissions from the dissolution of galvanic anodes in OWFs. This might be also caused by the high known sea bed dynamics in the German Bight (Zeiler et al., 2008), which results also in the spatial transport and dispersion of fresh pollutant-loaded sediments. Therefore, further investigations should be conducted in the future regarding the distributions of elemental mass fractions within and around OWFs in the investigated areas. This includes the ongoing monitoring of already well-studied sampling areas, but also modelling of natural and anthropogenic sediment relocation.

4.3. Possible source assignments

As discussed in chapter 4.1 and 4.2 area N-4 exhibits larger spatial and temporal variations of elemental mass fractions than the other investigated areas. To find possible explanations the analysis of Sr isotope amount ratios was included in this study. The isotopic composition of $n(^{87}Sr)/n(^{86}Sr)$ (median of OWFs ranging between 0.7144 and 0.7160) of the area N-4 north of Heligoland is comparable to sediments of the Elbe estuary (0.7143 to 0.7240 (Reese et al., 2019)) as shown in Fig. 3A, indicating sediment transport from the Elbe estuary along the residual current (Böhnecke, 1922) into the sampling area (area N-4). This suggests that elemental mass fractions of sediments north of Heligoland are influenced by riverine inputs of the river Elbe, besides other anthropogenic impacts such as the known dumping activities as well as the general high frequent ship traffic in this region (Ducrotoy et al., 2000).

In order to gain more insights from the elemental data regarding influences of different sediment origins, Ga/In ratios were calculated and compared to the Ga/In of the galvanic anodes. Fig. 5A shows that Ga/In ratios of Al anodes (0.44 ± 0.01 to 0.58 ± 0.02 (Reese et al., 2020)) are significantly different from Ga/In ratios of the UCC (313 ± 41 (Rudnick and Gao, 2003)), as well as the range of the Ga/In ratios of recent North Sea sediments as reported by Klein et al. (2022a) (62 to

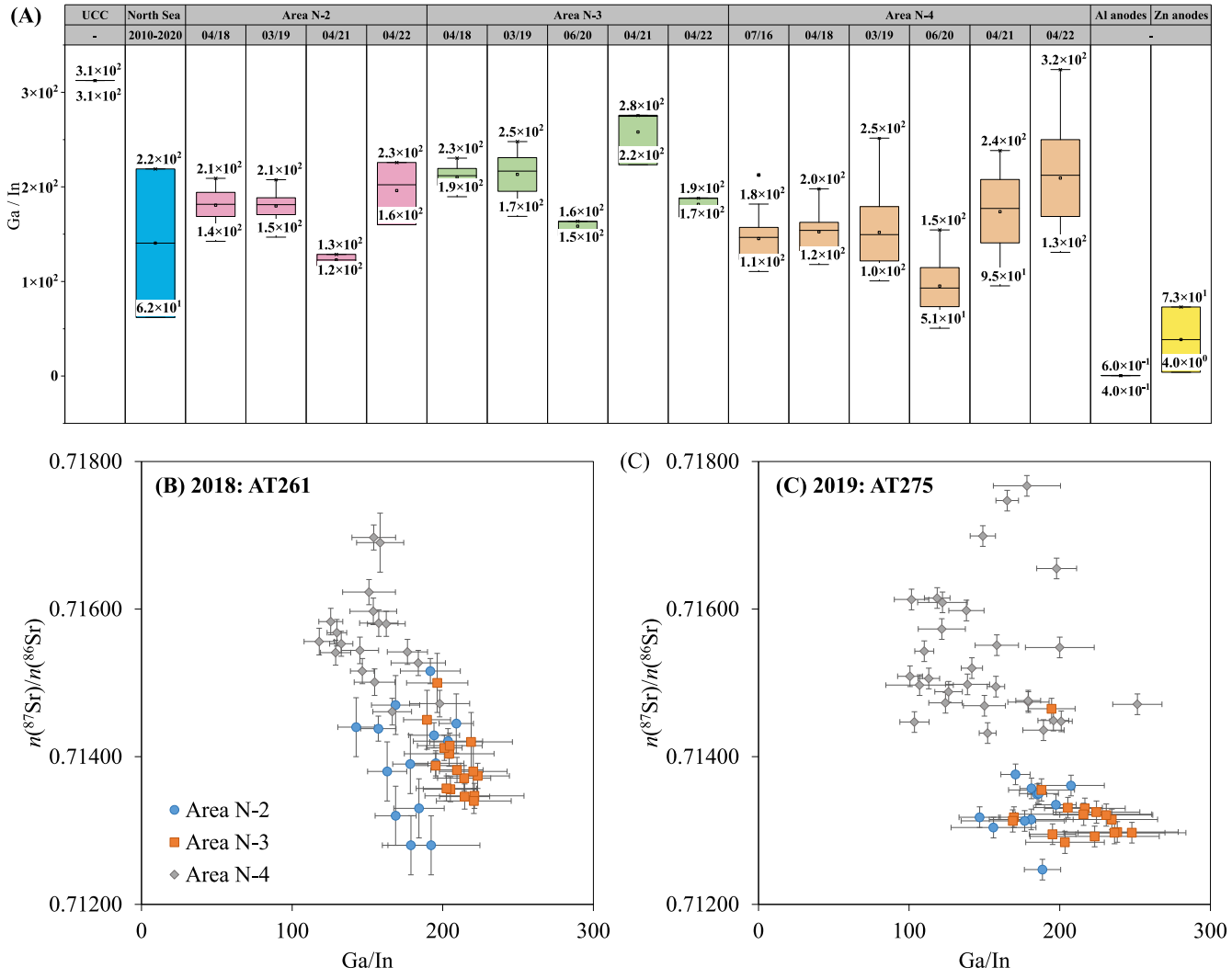

Fig. 5. A) Element ratio Ga/In in North Sea sediments in and around OWFs of the German Bight taken between 2016 and 2020 together with Ga/In for UCC (Rudnick and Gao, 2003), North Sea sediments between 2010 and 2020 (Klein et al., 2022a) and galvanic anodes (Reese et al., 2020). B) Isotope ratio $n(^{87}Sr)/n(^{86}Sr)$ plotted against the element ratio Ga/In for the sediments samples taken in 2018 and (C) 2019. Error bars correspond to expanded uncertainties $U(k = 2)$ for isotope ratios and to combined uncertainties $U(k = 1)$ for Ga/In.

219). Therefore, possible anthropogenic influences of dissolving anodes should result in lower Ga/In of the sediment samples. Indeed, measured Ga/In ratios of this study are mostly within the reference range of Klein et al. (2022a). Solely the areas N-3 (2021) and N-4 (2022) show Ga/In ratios exceeding this given reference range. Currently, Ga/In ratios of the analyzed sediment samples do not suggest sufficiently large anthropogenic inputs of Ga or In to significantly alter Ga/In ratios. The plot of $n(^{87}Sr)/n(^{86}Sr)$ against Ga/In in Fig. 5B shows, that the sediments of area N-4 form a distinct group indicating a different sediment type and therefore a different origin compared to other investigated areas which is in good agreement to the conclusions based on Sr isotope amount ratio analysis.

5. Conclusion

The data shows that mass fractions of the selected tracer elements in the sediment are currently predominantly within the range of the known variability in the study areas. Locally elevated mass fractions were for Pb and Cd. For the first time, data could be generated for the tracers In and Ga in OWFs in the German Bight.

The high dynamics in the area and the associated large-scale water and particulate matter exchange contribute to the measured mass fractions that were mostly within the range of the known variability for the German Bight. Based on the Ga and In elemental mass fraction data and the prevailing dilution and distribution processes, there are currently no direct effects discernible due to the use of galvanic anodes. For a better source allocation sound geogenic background levels for emerging contaminants are necessary, which are currently lacking for the North Sea. In addition, limited information about the biogeochemistry of Ga and In is currently available. However, due to the specific situation in the German Bight in terms of historical pollution, a wide range of anthropogenic sources and highly dynamic environmental processes, it is currently very challenging to fully differentiate the additional pollution load caused by OWFs.

Due to the continuous operation and development of offshore wind energy, the chemical emissions from corrosion protection will further increase keeping in mind the planned development e.g. for the German EEZ (30 GW until 2030) as well as the entire EU North Sea area (300 GW until 2050). To measure the metal input from galvanic anodes as well as the general operation we propose to continue the monitoring of the tracer elements in order to trace possible emissions by OWFs. Moreover, we suggest the application of Ga/In and potentially other element ratios as further tool, as the Ga/In ratio from galvanic anodes differentiates greatly from Ga/In in North Sea sediments. Sr isotope amount ratios can help to differentiate geogenic from anthropogenic signals and account for differences in sediment types.

Although the study cannot proof the direct impact of OWF emissions on environmental concentrations, around 13 years after the operational start of the first OWF within the German Bight, it is clear that galvanic anodes are per se a continuous source of metal emissions and thus are a new source of pollution within the marine environment. Further investigations should contribute to better assess possible medium- to long-term effects of such chemical emissions on the marine environment. Based on long-term monitoring of the critical elements, possible accumulations caused by the corrosion protection of offshore installations could be observed and evaluated in the future. Furthermore, future OWF projects should also consider alternative corrosion protections techniques during their planning to reduce chemical emissions.

Funding

This work was supported by the BSH through the projects OffChEm I and II (BSH contract codes: 10036781 and 10052123, Hereon contract codes: 17/2017 and 169/2021) and by the German Federal Ministry for Digital and Transport (BMDV) in the context of the BMDV Network of Experts.

Ole Klein was funded by the European Metrology Program for Innovation and Research (EMPIR) project MetroCycleEU (Funder ID: 10.13039/100014132, Grant number: 20IND01 MetroCycleEU).

CRediT authorship contribution statement

Anna Ebeling: Methodology, Validation, Investigation, Data curation, Writing – original draft, Visualization. **Dominik Wippermann:** Validation, Investigation, Data curation, Writing – original draft, Visualization. **Tristan Zimmermann:** Methodology, Investigation, Writing – original draft. **Ole Klein:** Investigation, Data curation, Writing – review & editing, Visualization. **Torben Kirchgeorg:** Conceptualization, Investigation, Project administration, Writing – review & editing. **Ingo Weinberg:** Conceptualization, Project administration, Writing – review & editing. **Simone Hasenbein:** Investigation, Writing – review & editing. **Anna Plaß:** Investigation, Writing – review & editing. **Daniel Pröfrock:** Conceptualization, Investigation, Writing – review & editing, Project administration, Funding acquisition.

Declaration of competing interest

The authors declare the following financial interests/personal relationships which may be considered as potential competing interests:

Anna Ebeling reports financial support was provided by Federal Maritime and Hydrographic Agency. Dominik Wippermann reports financial support was provided by Federal Maritime and Hydrographic Agency. This work was supported by the BSH through the projects OffChEm I and II (BSH contract codes: 10036781 and 10052123, Hereon contract codes: 17/2017 and 169/2021) and by the German Federal Ministry for Digital and Transport (BMDV) in the context of the BMDV Network of Experts. Ole Klein was funded by the European Metrology Program for Innovation and Research (EMPIR) project MetroCycleEU (Funder ID: 10.13039/100014132, Grant number: 20IND01 MetroCycleEU).

Data availability

Data will be made available on request.

Acknowledgements

We thank Nathalie Voigt, Catharina Petrauskas, Bettina Rust, Andrea Pieper and Svenja Faust for their support in the lab and preparations of sampling campaigns. Bettina Rust, Nathalie Voigt, Johanna Irrgeher, Andrea Pieper, Lisett Kretzschmann, Svenja Faust, Marcel Herbst, Simon Tewes, Francisco de la Granda Grandoso, Burkhard Erbslöh and Fadi el Gareb are acknowledged for help during the sampling campaigns. We thank Carlotta Pehlke and Jonas Ludwig for their help to analyze isotope ratios of Sr. The anonymous reviewers are acknowledged for their feedback. Further, we would like to thank both crews of the research vessels Atair (BSH) and Ludwig Prandtl (Hereon).

Appendix A. Supplementary data

Supplementary data to this article can be found online at https://doi.org/10.1016/j.marpolbul.2023.115396.

References

Ackermann, F., Bergmann, H., Schleichert, U., 1983. Monitoring of heavy metals in coastal and estuarine sediments - a question of grain-size: <20 μm versus <60 μm. Environ. Technol. Lett. 4, 317–328. https://doi.org/10.1080/09593338309384212.

Andrews, M.G., Jacobson, A.D., Lehn, G.O., Horton, T.W., Craw, D., 2016. Radiogenic and stable Sr isotope ratios (87Sr/86Sr, δ88/86Sr) as tracers of riverine cation sources and biogeochemical cycling in the Milford Sound region of Fiordland, New Zealand. Geochim. Cosmochim. Acta 173, 284–303. https://doi.org/10.1016/j.gca.2015.10.005.

Barbarin, M., Turquois, C., Dubillot, E., Huet, V., Churlaud, C., Muttin, F., Thomas, H., 2023. First quantitative biomonitoring study of two ports (marina, commerce) in French littoral area: evaluation of metals released into the marine environment and resulting from galvanic anodes. Sci. Total Environ. 857, 159244 https://doi.org/10.1016/j.scitotenv.2022.159244.

Bayon, G., Freslon, N., Germain, Y., Bindeman, I.N., Trinquier, A., Barrat, J.-A., 2021. A global survey of radiogenic strontium isotopes in river sediments. Chem. Geol. 559, 119958 https://doi.org/10.1016/j.chemgeo.2020.119958.

Bell, A.M., von der Au, M., Regnery, J., Schmid, M., Meermann, B., Reifferscheid, G., Ternes, T., Buchinger, S., 2020. Does galvanic cathodic protection by aluminum anodes impact marine organisms? Environ. Sci. Eur. 32, 157. https://doi.org/10.1186/s12302-020-00441-3.

Böhnecke, G., 1922. Salzgehalt und Strömungen der Nordsee. Zeitschrift der Gesellschaft für Erdkunde zu Berlin 300–302.

Boyle, E., Lee, J.-M., Echegoyen, Y., Noble, A., Moos, S., Carrasco, G., Zhao, N., Kayser, R., Zhang, J., Gamo, T., Obata, H., Norisuye, K., 2014. Anthropogenic lead emissions in the ocean: the evolving global experiment. Oceanography 27, 69–75. https://doi.org/10.5670/oceanog.2014.10.

Brand, W.A., Coplen, T.B., Vogl, J., Rosner, M., Prohaska, T., 2014. Assessment of interna- tional reference materials for isotope-ratio analysis (IUPAC technical report). Pure Appl. Chem. 86, 425–467.

Brückner, S., Mackensen, A., 2006. Deep-water renewal in the Skagerrak during the last 1200 years triggered by the North Atlantic oscillation: evidence from benthic foraminiferal δ8O. The Holocene 16, 331–340. https://doi.org/10.1191/0959683605hl931rp.

BSH, 1991. Jahresbericht 1990. Hamburg. https://digitale-bibliothek.bsh.de/viewer/image/62589/5/.

BSH, 2009. System Nordsee – Zustand 2005 Im Kontext Langzeitlicher Entwicklungen (System North Sea - State 2005 in the Context of Long-Term Developments). Hamburg & Rostock.

BSH, 2016. Nordseezustand 2008–2011. Hamburg & Rostock. https://www.bsh.de/DE/PUBLIKATIONEN/_Anlagen/Downloads/Meer_und_Umwelt/Berichte-des-BSH/Beri1chte-des-BSH_54.html.

BSH, 2023. Flächenentwicklungsplan 2023 für die deutsche Nordsee und Ostsee. Hamburg & Rostock. https://www.bsh.de/DE/THEMEN/Offshore/Meeresfachplanung/Flaechenentwicklungsplan/_Anlagen/Downloads/FEP_2023_1/Flaechenentwicklungsplan_2023.pdf?__blob=publicationFile&v=1.

Caplat, C., Oral, R., Mahaut, M.L., Mao, A., Barillier, D., Guida, M., Della Rocca, C., Pagano, G., 2010. Comparative toxicities of aluminum and zinc from sacrificial anodes or from sulfate salt in sea urchin embryos and sperm. Ecotoxicol. Environ. Saf. 73, 1138–1143. https://doi.org/10.1016/j.ecoenv.2010.06.024.

Caplat, C., Mottin, E., Lebel, J.-M., Serpentini, A., Barillier, D., Mahaut, M.-L., 2012. Impact of a sacrificial anode as assessed by zinc accumulation in different organs of the oyster Crassostrea gigas: results from Long- and short-term laboratory tests. Arch. Environ. Contam. Toxicol. 62, 638–649. https://doi.org/10.1007/s00244-011-9737-0.

Caplat, C., Basuyaux, O., Pineau, S., Deborde, J., Grolleau, A.M., Leglatin, S., Mahaut, M. L., 2020. Transfer of elements released by aluminum galvanic anodes in a marine sedimentary compartment after long-term monitoring in harbor and laboratory environments. Chemosphere 239, 124720. https://doi.org/10.1016/j.chemosphere.2019.124720.

Capo, R.C., Stewart, B.W., Chadwick, O.A., 1998. Strontium isotopes as tracers of ecosystem processes: theory and methods. Geoderma 82, 197–225.

Carpenter, J.R., Merckelbach, L., Callies, U., Clark, S., Gaslikova, L., Baschek, B., 2016. Potential impacts of offshore wind farms on North Sea stratification. PLoS One 11, e0160830. https://doi.org/10.1371/journal.pone.0160830.

Christiansen, N., Daewel, U., Djath, B., Schrum, C., 2022. Emergence of large-scale hydrodynamic structures due to atmospheric offshore wind farm wakes. Front. Mar. Sci. 9 https://doi.org/10.3389/fmars.2022.818501.

Coplen, T.B., 2011. Guidelines and recommended terms for expression of stable-isotope-ratio and gas-ratio measurement results. Rapid Commun. Mass Spectrom. 25, 2538–2560. https://doi.org/10.1002/rcm.5129.

de Laeter, J.R., Böhlke, J.K., De Bièvre, P., Hidaka, H., Peiser, H.S., Rosman, K.J.R., Taylor, P.D.P., 2003. Atomic weights of the elements. Review 2000 (IUPAC technical report). Pure Appl. Chem. 75, 683–800. https://doi.org/10.1351/pac200375060683.

Environmental impacts of offshore wind farms in the Belgian part of the North Sea. Attraction, avoidance and habitat use at various spatial scales. In: Degraer, S., Brabant, R., Rumes, B., Vigin, L. (Eds.), 2021. Royal Belgian Institute of Natural Sciences, OD Natural Environment. Marine Ecology and Management, Brussels.

Deng, F., Hellmann, S., Zimmermann, T., Pröfrock, D., 2021. Using Sr-Nd-Pb isotope systems to trace sources of sediment and trace metals to the Weser River system (Germany) and assessment of input to the North Sea. Sci. Total Environ. 791, 148127 https://doi.org/10.1016/j.scitotenv.2021.148127.

DIN e.V, 2006. DIN ISO 11843-2:2006-06: Capability of detection - Part 2: Methodology in the Linear Calibration Case.

DIN e.V, 2008. DIN 32645:2008-11: Chemical Analysis - Decision Limit, Detection Limit and Determination Limit Under Repeatability Conditions - Terms, Methods, Evaluation. https://doi.org/10.31030/1465413.

Ducrotoy, J.P., Elliott, M., de Jonge, V.N., 2000. The North Sea. Mar. Pollut. Bull. 41 (1), 5–23. https://doi.org/10.1016/S0025-326X(00)00099-0.

ECHA, 2020. Indium - registration dossier. available online at. https://echa.europa.eu/de/registration-dossier/-/registered-dossier/22264/6/1.

EURACHEM/CITAC, 2012. EURACHEM/CITAC guide: Quantifying Uncertainty in Analytical Measurements, 3 https://www.eurachem.org/images/stories/Guides/pdf/QUAM2012_P1.pdf.

Filella, M., Rodriguez-Murillo, J.C., 2017. Less-studied TCE: are their environmental concentrations increasing due to their use in new technologies? Chemosphere 182, 605–616. https://doi.org/10.1016/j.chemosphere.2017.05.024.

Forster, R.M., 2018. The effect of monopile-induced turbulence on local suspended sediment pattern around UK wind farms: field survey report. In: An IECS report to The Crown Estate. Hull.

Gabelle, C., Baraud, F., Biree, L., Gouali, S., Hamdoun, H., Rousseau, C., van Veen, E., Leleyter, L., 2012. The impact of aluminium sacrificial anodes on the marine environment: a case study. Appl. Geochem. 27, 2088–2095. https://doi.org/10.1016/j.apgeochem.2012.07.001.

Golding, L.A., Angel, B.M., Batley, G.E., Apte, S.C., Krassoi, R., Doyle, C.J., 2015. Derivation of a water quality guideline for aluminium in marine waters. Environ. Toxicol. Chem. 34, 141–151. https://doi.org/10.1002/etc.2771.

Horsky, M., Irrgeher, J., Prohaska, T., 2016. Evaluation strategies and uncertainty calculation of isotope amount ratios measured by MC ICP-MS on the example of Sr. Anal. Bioanal. Chem. 408, 351–367. https://doi.org/10.1007/s00216-015-9003-9.

Kirchgeorg, T., Weinberg, I., Hörnig, M., Baier, R., Schmid, M.J., Brockmeyer, B., 2018. Emissions from corrosion protection systems of offshore wind farms: evaluation of the potential impact on the marine environment. Mar. Pollut. Bull. 136, 257–268. https://doi.org/10.1016/j.marpolbul.2018.08.058.

Klein, O., Zimmermann, T., Ebeling, A., Kruse, M., Kirchgeorg, T., Pröfrock, D., 2022a. Occurrence and temporal variation of technology-critical elements in North Sea sediments-a determination of preliminary reference values. Arch. Environ. Contam. Toxicol. 82, 481–492. https://doi.org/10.1007/s00244-022-00929-4.

Klein, O., Zimmermann, T., Hildebrandt, L., Profrock, D., 2022b. Technology-critical elements in Rhine sediments - a case study on occurrence and spatial distribution. Sci. Total Environ. 852, 158464 https://doi.org/10.1016/j.scitotenv.2022.158464.

Komarek, M., Ettler, V., Chrastny, V., Mihaljevic, M., 2008. Lead isotopes in environmental sciences: a review. Environ. Int. 34, 562–577. https://doi.org/10.1016/j.envint.2007.10.005.

Kragten, J., 1994. Tutorial review. Calculating standard deviations and confidence intervals with a universally applicable spreadsheet technique. Ana 119, 2161. https://doi.org/10.1039/an9941902161.

Kremling, K., Andreae, M.O., Brgmann, L., van den Berg, C.M.G., Prange, A., Schirmacher, M., Koroleff, E., Kremling, K., Kus, J., 1999. Determination of trace elements. In: Grasshoff, K., et al. (Eds.), Methods of Seawater Analysis. Wiley-VCH Verlag GmbH, Weinheim, Germany, pp. 253–364. https://doi.org/10.1002/9783527613984.ch12.

Larsen, M.M., Blusztajn, J.S., Andersen, O., Dahllof, I., 2012. Lead isotopes in marine surface sediments reveal historical use of leaded fuel. J. Environ. Monit. 14, 2893–2901. https://doi.org/10.1039/c2em30579h.

Levallois, A., Caplat, C., Basuyaux, O., Lebel, J.M., Laisney, A., Costil, K., Serpentini, A., 2022. Effects of chronic exposure of metals released from the dissolution of an aluminium galvanic anode on the Pacific oyster Crassostrea gigas. Aquat. Toxicol. 249, 106223 https://doi.org/10.1016/j.aquatox.2022.106223.

Macdonald, D.D., Carr, R.S., Calder, F.D., Long, E.R., Ingersoll, C.G., 1996. Development and evaluation of sediment quality guidelines for Florida coastal waters. Ecotoxicology 5, 253–278. https://doi.org/10.1007/BF00118995.

Mao, A., Mahaut, M.-L., Pineau, S., Barillier, D., Caplat, C., 2011. Assessment of sacrificial anode impact by aluminum accumulation in mussel Mytilus edulis: a large-scale laboratory test. Mar. Pollut. Bull. 62, 2707–2713. https://doi.org/10.1016/j.marpolbul.2011.09.017.

Mottin, E., Caplat, C., Latire, T., Mottier, A., Mahaut, M.-L., Costil, K., Barillier, D., Lebel, J.-M., Serpentini, A., 2012. Effect of zinc sacrificial anode degradation on the defence system of the Pacific oyster, Crassostrea gigas: chronic and acute exposures. Mar. Pollut. Bull. 64, 1911–1920. https://doi.org/10.1016/j.marpolbul.2012.06.017.

Nham, N., 2017. Evaluation of Different Sieving Methods for the Extraction of the Fine Sediment Fraction and their Influence on the Elemental and Isotopic Fingerprint. Universität Hamburg.

OSPAR, 2009. Losses of contaminants from ships' coatings and anodes. https://qsr2010.ospar.org/media/assessments/p00462_Leaching_report.pdf.

OSPAR, 2010. Hazardous Substances, Quality Status Report 2010. OSPAR Commission, Lodnon, pp. 37–52.

Peganova, S., Eder, K., 2004. Zinc. In: Merian, E., Anke, M., Ihnat, M., Stoeppler, M. (Eds.), Elements and Their Compounds in the Environment: Occurrence, Analysis and Biological Relevance, second ed. Wiley-VCH, Weinheim, p. 1203e1239.

Pickaver, A.H., 1982. Titanium dioxide waste dumping at sea time to call a halt. Mar. Pollut. Bull. 13, 375–379. https://doi.org/10.1016/0025-326x(82)90110-2.

Pröfrock, D., Prange, A., 2012. Inductively coupled plasma-mass spectrometry (ICP-MS) for quantitative analysis in environmental and life sciences: a review of challenges, solutions, and trends. Appl. Spectrosc. 66, 843–868. https://doi.org/10.1366/12-06681.

Reese, A., Zimmermann, T., Pröfrock, D., Irrgeher, J., 2019. Extreme spatial variation of Sr, Nd and Pb isotopic signatures and 48 element mass fractions in surface sediment of the Elbe River estuary - suitable tracers for processes in dynamic environments? Sci. Total Environ. 668, 512–523. https://doi.org/10.1016/j.scitotenv.2019.02.401.

Reese, A., Voigt, N., Zimmermann, T., Irrgeher, J., Pröfrock, D., 2020. Characterization of alloying components in galvanic anodes as potential environmental tracers for heavy metal emissions from offshore wind structures. Chemosphere 257, 127182. https://doi.org/10.1016/j.chemosphere.2020.127182.

Retzmann, A., Zimmermann, T., Pröfrock, D., Prohaska, T., Irrgeher, J., 2017. A fully automated simultaneous single-stage separation of Sr, Pb, and Nd using DGA resin for the isotopic analysis of marine sediments. Anal. Bioanal. Chem. 409, 5463–5480. https://doi.org/10.1007/s00216-017-0468-6.

Romero-Freire, A., Santos-Echeandía, J., Neira, P., Cobelo-García, A., 2019. Less-studied technology-critical elements (Nb, Ta, Ga, In, Ge, Te) in the marine environment: review on their concentrations in water and organisms. Front. Mar. Sci. 6 https://doi.org/10.3389/fmars.2019.00532.

Rousseau, C., Baraud, F., Leleyter, L., Gil, O., 2009. Cathodic protection by zinc sacrificial anodes: impact on marine sediment metallic contamination. J. Hazard. Mater. 167, 953–958. https://doi.org/10.1016/j.jhazmat.2009.01.083.

Rudnick, R.L., Gao, S., 2003. Composition of the Continental Crust, pp. 1–64. https://doi.org/10.1016/b0-08-043751-6/03016-4.

Sarker, I., Moore, L.R., Tetu, S.G., 2021. Investigating zinc toxicity responses in marine Prochlorococcus and Synechococcus. Microbiology 167. https://doi.org/10.1099/mic.0.001064.

Stenton, C.A., Bolger, E.L., Michenot, M., Dodd, J.A., Wale, M.A., Briers, R.A., Hartl, M.G. J., Diele, K., 2022. Effects of pile driving sound playbacks and cadmium co-exposure on the early life stage development of the Norway lobster, *Nephrops norvegicus*. Mar. Pollut. Bull. 179, 113667 https://doi.org/10.1016/j.marpolbul.2022.113667.

Voet, H.E.E., Van Colen, C., Vanaverbeke, J., 2022. Climate change effects on the ecophysiology and ecological functioning of an offshore wind farm artificial hard substrate community. Sci. Total Environ. 810, 152194 https://doi.org/10.1016/j.scitotenv.2021.152194.

von der Au, M., Zimmermann, T., Kleeberg, U., von Tümpling, W., Pröfrock, D., 2022. Characteristic regional differences in trace element pattern of 2014 German North Sea surface Wadden sediments - a judge and assessment. Mar. Pollut. Bull. 184, 114208 https://doi.org/10.1016/j.marpolbul.2022.114208.

Wang, T., Zou, X., Li, B., Yao, Y., Li, J., Hui, H., Yu, W., Wang, C., 2018. Microplastics in a wind farm area: a case study at the Rudong Offshore Wind Farm, Yellow Sea, China. Mar. Pollut. Bull. 128, 466–474. https://doi.org/10.1016/j.marpolbul.2018.01.050.

Wang, T., Ru, X., Deng, B., Zhang, C., Wang, X., Yang, B., Zhang, L., 2023. Evidence that offshore wind farms might affect marine sediment quality and microbial communities. Sci. Total Environ. 856, 158782 https://doi.org/10.1016/j.scitotenv.2022.158782.

Wiederhold, J.G., 2015. Metal stable isotope signatures as tracers in environmental geochemistry. Environ. Sci. Technol. 49, 2606e2624. https://doi.org/10.1021/es504683e.

WindEurope, 2022. Wind energy in Europe: 2021 Statistics and the outlook for 2022–2026. In: https://proceedings.windeurope.org/biplatform/rails/active_storage/blobs/eyJfcmFpbHMiOnsibWVzc2FnZSI6IkJBaHBBbFFEIiwiZXhwIjpudWxsLCJwdXIiOiJibG9iX2lkIn19–f507a22c9854863e01fd427239f10167d031cc66/Windeurope-Wind-energy-in-Europe-2021-statistics.pdf.

Wright, A.J., Araujo-Wang, C., Wang, J.Y., Ross, P.S., Tougaard, J., Winkler, R., Marquez, M.C., Robertson, F.C., Williams, K.F., Reeves, R.R., 2020. How 'blue' is 'green' energy? Trends Ecol. Evol. 35, 235–244. https://doi.org/10.1016/j.tree.2019.11.002.

Zeiler, M., Schwarzer, K., Bartholomä, A., Ricklefs, K., 2008. Seabed morphology and sediment dynamics. In: Kuratorium für Forschung im Küsteningenieurwesen (Ed.), Die Küste. Archive for Research and Technology on the North Sea and Baltic Coast, pp. 31–41, 74 ICCE. https://hdl.handle.net/20.500.11970/101589.

Zimmermann, T., Mohamed, A.F., Reese, A., Wieser, M.E., Kleeberg, U., Pröfrock, D., Irrgeher, J., 2019a. Zinc isotopic variation of water and surface sediments from the German Elbe River. Sci. Total Environ. 135219 https://doi.org/10.1016/j.scitotenv.2019.135219.

Zimmermann, T., Retzmann, A., Schober, M., Pröfrock, D., Prohaska, T., Irrgeher, J., 2019b. Matrix separation of Sr and Pb for isotopic ratio analysis of Ca-rich samples via an automated simultaneous separation procedure. Spectrochim. Acta B 151, 54–64. https://doi.org/10.1016/j.sab.2018.11.009.

Zimmermann, T., von der Au, M., Reese, A., Klein, O., Hildebrandt, L., Pröfrock, D., 2020. Substituting HF by HBF4- an optimized digestion method for multi-elemental sediment analysis via ICP-MS/MS. Anal. Methods 12, 3778–3787. https://doi.org/10.1039/d0ay01049a.